Building vulnerability and seismic risk analysis in the urban area of Mt. Etna volcano (Italy)

S. D'Amico[1], F. Meroni[1], M.L. Sousa[2], and G. Zonno[1]

[1] Istituto Nazionale di Geofisica e Vulcanologia, Italy

[2] Laboratório Nacional de Engenharia Civil, Portugal

Corresponding author: salvatore.damico@ingv.it

Abstract

The tectonic system of the eastern flank of Mt. Etna volcano (Sicily, Italy) is the source of most of the strongest earthquakes occurring in the area over the last 205 years. A total of 12 events with epicentre intensities ≥ VIII EMS have occurred at Mt. Etna, 10 of which were located on the eastern flank. This indicates a mean recurrence time of about 20 years. This area is highly urbanised, with many villages around the volcano at altitudes up to 700 m a.s.l. The southern and eastern flanks are particularly highly populated areas, with numerous villages very close to each other.

The probabilistic seismic hazard due to local faults for Mt. Etna was calculated by adopting a site approach to seismic hazard assessment. Only the site histories of local volcano-tectonic earthquakes were considered, leaving out the effects due to strong regional earthquakes that occurred in north-eastern and south-eastern Sicily.

The inventory used in this application refers to residential buildings. These data were extracted from the 1991 census of the Italian National Institute of Statistics, and are grouped according to the census sections. The seismic vulnerability of the elements at risk belonging to a given building typology is described by a vulnerability index, in accordance with a damage model based on macroseismic intensities.

For the estimation of economic losses due to physical damage to buildings, an integrated impact indicator was used, which is equivalent to the lost building volume. The expected annualised economic earthquake losses were evaluated both in absolute and in relative terms, and were compared with the geographical distribution of seismic hazard and with similar evaluations of losses for other regions.

Keywords: economic losses, Mt. Etna volcano, seismic risk, vulnerability,

1. Introduction

The problem of seismic risk is a well-known issue at Mt. Etna (Sicily, Italy) due to the high-intensity volcano–tectonic earthquakes that frequently damage the highly populated flanks of this volcano. Indeed, the Mt. Etna region is also affected by strong regional events ($6.6 \leq M \leq 7.4$), such as the major Val di Noto earthquakes in 1169 and 1693, the 1818 Etnean earthquake, and the 1908 Messina earthquake (Rovida et al. 2011). Moreover, this area is also exposed to local earthquakes that albeit of lower magnitude ($M \leq 4.9$), can produce severe damage and even destruction (Azzaro 2004). These earthquakes may have epicentral intensities, I_0, that reach up to X EMS-98 (Grünthal 1998), because of the particularly shallow foci (≤ 3 km) (Azzaro 2004). Volcano-tectonic events are very frequent, with 167 shocks exceeding the damage threshold ($I_0 >$ V EMS-98) over the last 181 years. These are largely located on the eastern flank of Mt. Etna volcano, which is traversed by a dense network of seismogenic faults. Urbanisation is particularly high on the southern and eastern flanks, where many villages are located up to 700 m a.s.l., another element that potentially contributes to the high earthquake risk level of the area.

In the framework of the UPStrat-MAFA project, the assessment of seismic risk on an urban scale through approaches and tools common to the studied areas (Zonno et al. 2012) has been applied to Mt. Etna. In this area, the assessment of seismic hazard, of probabilistic seismic scenarios and of buildings vulnerability, has enabled estimating risk in terms of annualised economic losses and degree of the earthquake impact on urbanized areas considered as a complex system of infrastructural networks (Meroni et al. 2015).

The aim of the present study is to estimate the order of magnitude of the risk associated with seismic losses in residential buildings on the eastern flank of Mt. Etna volcano. The results are given in terms of two interrelated risk indicators: the Annualised Economic earthquake Loss (*AEL*), and the Annualised Economic earthquake Loss Ratio (*AELR*).

These risk indicators were obtained in a similar way to what was done in FEMA (2008), although different ways to spell out the acronyms are used in the present study. In FEMA (2008), *AEL* is the acronym for Annualised Earthquake Loss and stands for the mean losses per year, based on building damages, and *AELR* is the acronym for Annualised Earthquake Loss Ratio and is defined as the ratio between *AEL* and the replacement value of the building inventory. In this paper, the term Economic was added to both the acronyms for the sake of consistency with another study in this volume (Sousa and Campos Costa, 2015), where another risk indicator, the Annualised earthquake Human Loss (*AHL*), was computed in addition to *AEL*. Both *AEL* and *AHL* are estimates

of earthquake losses, but the former is based on building damages and on related repair costs and the latter is based on the average number of casualties per year.

2. Seismicity and hazard of Mt. Etna

Mt. Etna volcano is located in south-eastern Sicily (Italy) at the intersection of two active regional master faults, with its tectonic settings commonly interpreted as due to the interactions of regional tectonics and local-scale volcano-related processes (Lo Giudice et al. 1982; Lo Giudice and Rasà 1992; McGuire and Pullen 1989; Monaco et al. 1997). As in many similar areas, the main features of the seismicity of this volcanic area are the high frequency, moderate magnitude, and shallow focal depth (often less than 3 km) (Alparone et al. 2014). Even if the maximum magnitudes of these earthquakes do not generally exceed 4.9, the effects in the epicentral area can be destructive whenever intensities reach up to X EMS-98. Over a period of 181 years, 167 earthquakes have exceeded the damage threshold of EMS-98 (I_0 > V), of which 17 reached I_0 > VII (EMS-98), and 5 caused more or less extensive destruction, having and epicentral intensity I_0 > VIII (EMS-98). This means that on average, one earthquake damages the Etnean area every year, one earthquake causes severe damage every 12 years, and one earthquake causes destruction every 10 years.

The frequent seismicity of the Mt. Etna area (Fig. 1) is exceptionally well documented in a database of historical data that has described the seismic and volcanic activities of Mt. Etna in great detail and with continuity since the late 1600s. In particular, the macroseismic catalogue of Etnean earthquakes (CMTE 2014), covering the period from 1832 to 2013, together with its back-extension as far as the year 1600 by specific historical investigations (Azzaro and Castelli, 2015), provides a complete and homogeneous dataset that is useful to obtain an integral picture of the main seismicity over a significantly long time-span. This also allows investigating the space-time evolution of seismic sequences, and its possible relationships with the eruptive activity.

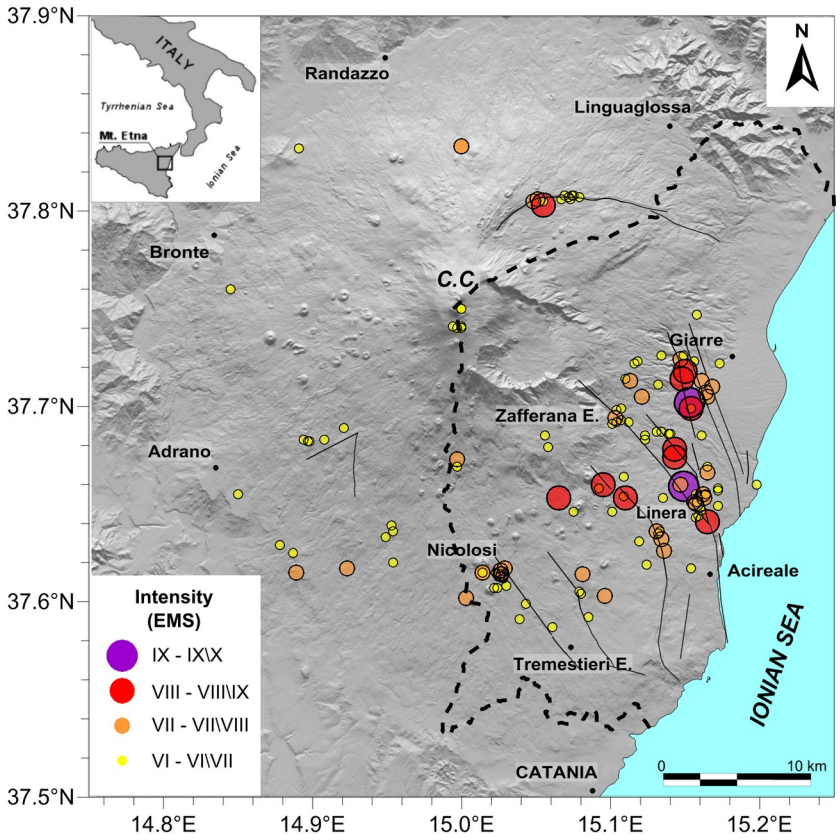

Figure 1. Location of the earthquakes with epicentral intensities ≥ VI EMS-98 in the Mt. Etna area from 1600 to 2013, according to the local macroseismic catalogue (CMTE 2014). Local seismogenic faults (Azzaro et al. 2013a) are shown as black lines; dashed line marks the study area.

The availability of this comprehensive database allows Probabilistic Seismic Hazard Assessment (PSHA) in terms of macroseismic intensity using as input macroseismic data. This approach (commonly indicated as the "site approach") has been specifically developed to handle this kind of data in a coherent statistical method that does not require any assumption about earthquake recurrence model and seismic source geometry (D'Amico and Albarello, 2008). During the last decade, PSHA studies using the site approach were performed in Italy and elsewhere (Mucciarelli et al. 2000; Albarello et al. 2002, 2007; D'Amico and Albarello 2003, 2008; Galea 2007; Bindi et al. 2012), and also for Mt. Etna (Azzaro et al. 2008, 2013b).

A detailed description of the results obtained in the framework of the UPStrat-MAFA project is given in Azzaro et al., 2015 (this volume). Recent probabilistic seismic hazard studies for Mt. Etna (Azzaro et al. 2008, 2013b) have shown that the hazard in the Etna region is controlled by the destructive regional earthquakes ($6.6 \leq M_W \leq 7.4$) and by local volcano-tectonic events; as the aim of the project was to investigate the risk associated with the volcano-tectonic seismicity, regional earthquakes occurring in the surrounding areas and that might have affected Mt. Etna have not been taken into account.

For a brief description, using the SASHA software of D'Amico and Albarello (2008), local seismic histories were compiled by combining the seismic effects observed at the sites during past earthquakes, and when needed, the 'virtual' intensities deduced from the epicentral data. This led to the acquisition of very comprehensive and detailed seismic histories and seismic sources available in the catalogue. A total of 4432 intensity datasets, related to 140 volcano-tectonic events that occurred from 1600 to 2013, were used. This combined dataset enabled reconstructing the seismic histories of 415 locations in the Mt. Etna region (53 municipalities, and 349 hamlets or minor settlements; 27 municipalities are located in the study area). To assess the seismic hazard (in terms of the probability that during a chosen future time span of length Δt the site under study will be shaken by at least one earthquake with local effects $\geq$ Is) SASHA evaluates the reliability of the seismic site histories and computes the seismic hazard at site. After fixing the probability threshold (the exceedance probability), the reference intensity, I_{ref}, is determined.

The probabilistic seismic hazard assessment map was computed using a grid with nodes spaced 1 km apart according to longitude and latitude. The final map for 50 years of exposure time with an exceedance probability of 10% shows the high level of hazard affecting the eastern flank of the volcano (Fig. 2). In particular, I_{ref} = VIII is confined to the south-eastern flank, and two small spots of I_{ref} = IX are along the main seismogenic faults of the volcano. Most of the Mt. Etna region shows a background of I_{ref} = VII, while the periphery of the volcano, which includes the town of Catania, is exposed to slightly damaging events (I_{ref} = VI).

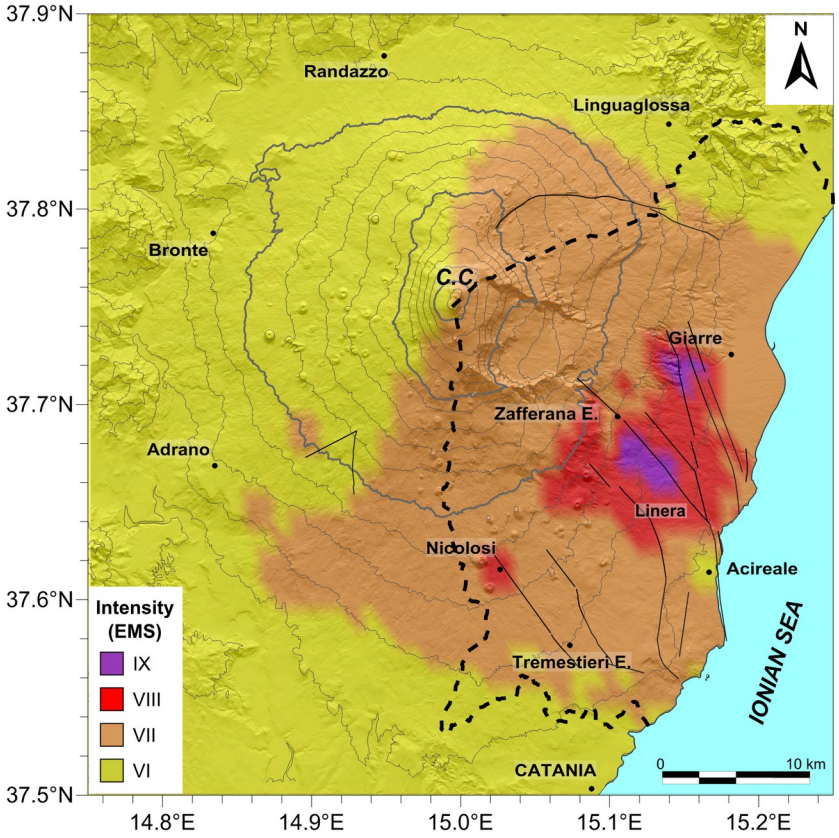

Figure 2. Hazard map for Mt. Etna. Expected intensity for a 10% exceedance probability in a 50 years exposure time period. Local seismogenic faults (Azzaro et al. 2013a) are shown as black lines; dashed line marks the study area

The return period related to each expected intensity for each node of the grid was calculated according to Equation (1):

$$Tr = -\frac{Te}{\ln(1 - P)} \qquad (1)$$

where *Tr* is the return period, *Te* is the exposure time, and P is the exceedance probability.

Figure 3 shows the expected intensities *versus* the return period for some of the locations; among these, some sites are expected to suffer effects larger or equal to VII, even for short return periods. A Beta theoretical distribution was fitted to these hazard curves to be used later in the seismic risk study made on the region (see chapter 4).

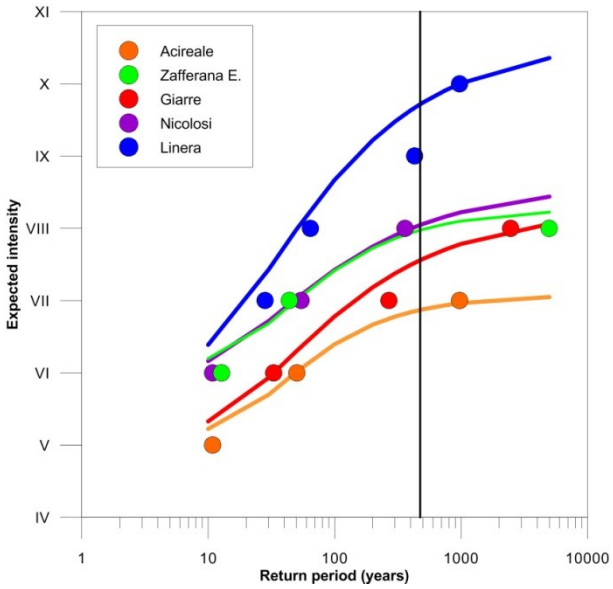

Figure 3. Expected intensity *versus* return period for some of the locations in Mt. Etna (circles) and related Beta theoretical distribution fitted to data (lines). The black vertical line marks the 475 years return period, which corresponds to a 10% exceedance probability in a 50 years exposure time period.

3. Vulnerability in the urban area of Mt. Etna

The study area covers part of the south-eastern flank of the Mt. Etna volcano, over an area of approximately 510 km^2, and includes 27 municipalities. It is worth noting that, in this study, the economic losses are exclusively based on residential building damage estimates and repair costs.

The inventory of the building stock has been taken from the data collected during the Italian census, which then has to be adapted appropriately to the entire Italian territory for the purposes of vulnerability assessment (Meroni et al. 1999, 2000). The data for the buildings were extracted from the 1991 Italian National Institute of Statistics (ISTAT) census (ISTAT 1991). The data were grouped according to the census sections, and vulnerability indices were determined using the approach proposed by Lagomarsino and Giovinazzi (2006), Giovinazzi and Lagomarsino (2001), and Bernardini et al. (2007).

According to this method, once a value has been fixed for building vulnerability (V) and given an intensity I, a mean damage grade (μ_D) can be determined using the following analytical function:

$$\mu_D = 2.5 + 3\tanh\left(\frac{I + 6.25V - 12.7}{3}\right) \times f(V, I) \qquad (2)$$

where $f(V_I, I)$ is defined as:

$$f(K,I) = \begin{cases} e^{\left[\frac{K}{2}\times(I-7)\right]} & I \le 7 \\ 1 & I > 7 \end{cases} \quad (3)$$

These census data are a primary source to assess residential building vulnerability over large areas. They provide a uniform coverage for the whole of Italy, making it possible to estimate the total number of buildings and their total volume. The ISTAT data on residential buildings allows defining the frequencies of groups of homogeneous structures with respect to a number of parameters that might influence their response to earthquakes, including vertical structures, age of construction, number of storeys, state of maintenance, and state of aggregation with adjacent buildings (see Table 1). Unfortunately, because of statistical privacy regulations, the most recent ISTAT census data (from the surveys in 2001 and 2011) only provide aggregated values, which constrain the vulnerability evaluation to rough estimations. The availability of such data solely in an aggregate form at a municipal level, without census section details and with few typological features on age, materials, building height, and other factors, mean they are not readily usable for vulnerability investigations (Crowley et al. 2009).

ISTAT was the direct source of information for the division of the total sum of the buildings into classes, according to the breakdown given in Table 1. The sub-division of the buildings according to the level of maintenance was based indirectly on the ISTAT data. Although the level of maintenance of a building is widely known to affect its behaviour under seismic conditions, the ISTAT data does not, unfortunately, provide such information. An analysis of the data collected revealed how the presence of effective installations' are is systematically associated with lower vulnerability indices than those with sub-standard installations. It was therefore decided to take the presence of effective systems as an indirect measurement of the state of maintenance of the buildings, and a further breakdown of the data into two classes was made on the basis of the information concerning the aspects of installations included in the ISTAT data. The sections of the census form considered were: "drinking water systems", "plumbing systems", "drainage systems", "connections to the sewage system", "bathtub and/or shower installations", "domestic hot water supply", and "fixed heating installations".

Table 1. **Typological classes of buildings identified from the ISTAT data.**

Structural typology	**Age**	**Number of floors**	**Location relative to adjacent buildings**	**Level of maintenance**
Masonry	pre-1919	1 or 2	Isolated	Good

Concrete – reinforced	1919 to 1945	3, 4 or 5	Block	Low
Concrete – soft-floor reinforced	1946 to 1960	6 or more		
Other typologies	1961 to 1971			
	1972 to 1981			
	post-1981			

Using the ISTAT data and adopting the methodology proposed by Lagomarsino and Giovinazzi (2006) and Giovinazzi and Lagomarsino (2001), seven distinct categories of buildings were initially identified: four with a masonry structural type (Table 2), and three with concrete structural type (Table 3). According to the other typology classes derived from the ISTAT data (i.e. age, floors, structural context, maintenance), the vulnerability index, I_v, of each category can be calibrated through appropriate behaviour modifiers. The given score can cause an increase or a decrease in the vulnerability index for the category, which is calculated in proportion to the number of buildings identified by that behaviour modifier, as inferred from Tables 2 and 3, through the behaviour modifiers summarised in Tables 4 and 5. The important factors for classifying the earthquake performance of buildings are presented in Tables 2, 3, 4 and 5. An increase in the I_v index indicates higher vulnerability factors.

Table 2. **Masonry buildings: identification of the categories based on the age of construction.**

Category	Building age	EMS98 typology	I_v
1	pre-1919	M1 – Rubble stone, fieldstone	50
		M3 – Simple stone	
		M5 – Bricks	
2	1919 to 1945	M3 – Simple stone	35
	urban area	M4 – Massive stone	
		M5 – Brick	
	1919 to 1945	M1 – Rubble stone, fieldstone	45
	rural area	M3 – Simple stone	
		M5 – Brick	
3	1946 to 1971	M3 – Simple stone	30
		M5 – Brick	
		M6 – Unreinforced masonry	
		with reinforced concrete floors	
4	post-1971	M6 - Unreinforced masonry	20
		with reinforced concrete floors	

I_v, vulnerability index

Table 3. **Reinforced concrete buildings: identification of the categories based on the age and typology of the construction.**

Category	Building age	EMS-98 typology	I_V
5	Before seismic code	RC1 – Frame in reinforced concrete (without ERD)	20
		RC4 – Concrete shear walls (without ERD)	
6	After seismic code	RC2 – Frame in reinforced concrete (moderate ERD)	0
		RC5 – Concrete shear walls (moderate ERD)	
7	Soft floor	Soft floor reinforced concrete buildings	40

ERD, earthquake-resistant design

I_v, vulnerability index

Table 4. Masonry buildings: assignment of scores for **the behaviour modifiers.**

Behaviour modifier	ISTAT classe	Score modifier for each category			
		Pre-1919	1919-1945	1946-1971	Post-1971
Level of maintenance	Low maintenance	+6	+6	+6	-
Number of floors	1 or 2 floors	-	-	-	-
	3, 4 or 5 floors	+5	+5	+5	+5
	6 or more floors	+10	+10	+10	+10
Structural context	Block of buildings	-	-	+6	+6

Table 5. **Concrete buildings: assignment of scores for the behaviour modifiers.**

Behavior modifier	ISTAT classes	Score modifier for each category
Building age	pre-1971	+6
Number of floors	1 or 2 floors	-6
	3, 4 or 5 floors	-
	6 or more floors	+6
Adjacent buildings without seismic design	Block of buildings	+6*

*, only for category 5 – buildings built before the seismic code

The scores chosen for these modifiers are consistent with data published in a study of vulnerability evaluation carried out over large areas of the Italian territory (Meroni et al. 2000). This study used the reference vulnerability forms (levels I and II) of the *Gruppo Nazionale per la Difesa dai Terremoti* (National Group for Defence against Earthquakes) to the municipalities for which

were available, and then evaluated the average vulnerability index for homogeneous groups of buildings according to the different ISTAT census classes. For example, for each age group of masonry buildings, it was possible to evaluate changes in the vulnerability index that depended on the number of floors, the structural context, and the level of maintenance.

From Frassine and Giovinazzi (2004), it is possible to derive the relationship which relates the above vulnerability index I_v used by GNDT method with a *V* index proposed by Lagomarsino and Giovinazzi (2006) and Bernardini et al. (2007), and adopted in this project for residential buildings in large areas.

Following the above-described approach, the seismic vulnerability index for each building typology was evaluated using the vulnerability index *V*, which varies between 0 and 1. This was defined by the weighted sum of the volumes for each of the vulnerability classes multiplied by the score of each vulnerability class. The geographic distribution of the average vulnerability index of residential buildings is shown in Figure 4. Multiple maps can be used to show the 'amount' (volume) of the buildings for each of the typological census classes (in theory this would give more than 360 maps). Figure 4 shows a parcelled pattern of the average building vulnerability due to the high number of different census sections. Furthermore, the only evident pattern from the map is the relative increase in the average building vulnerability index of the residential buildings along the coast.

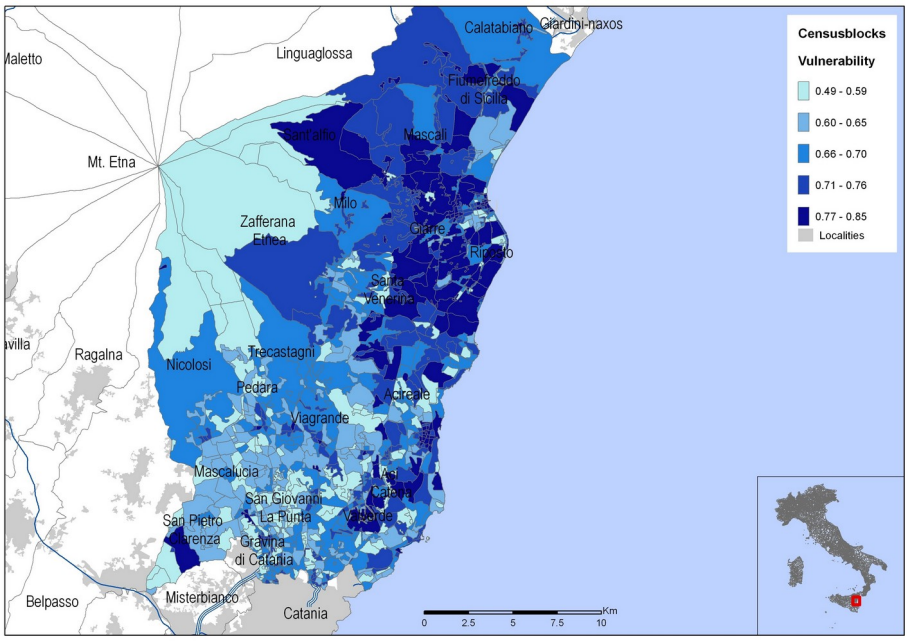

Figure 4. Average vulnerability index for each census section of the study area.

4. Seismic risk evaluation

For this application, we followed the approach for the probabilistic analysis of seismic risk shown in Figure 5 and in Equations (4) and (5) (adapted from Sousa 2008).

The probabilistic analysis of seismic risk is given by the Equation (4):

$$P(L>l) = \int_D \int_H P(L>l|d)\, P(D>d|h)\, f_H(h)\, dh\, dd \qquad (4)$$

where H, D and L are random variables representing seismic Hazard, Damage and Loss; $f_H(h)$ is the probability density function of seismic hazard; $P(D>d|h)$ is the exceedance probability distribution of damage conditional on hazard, i.e. the fragility curve; $P(L>l|d)$ is the exceedance probability distribution of loss conditional on damage and $P(L>l)$ is the exceedance distribution of loss.

This expression is graphically illustrated in Figure 5 for a building typology of vulnerability v; i.e. for a homogeneous group of elements at risk. Note that in Figure 5, each variable distribution was plotted with the same colour as in Equation (4). The probability density function of the seismic hazard is given by the green distribution in the 4th quadrant, then, for a given level of hazard the expected conditional damage value is obtained over a vulnerability curve plotted in blue in the 1st quadrant. The dispersion on damage inherent to building typologies is characterized by the fragility curve also plotted in blue in the 1st quadrant. The integration of the damage conditional distribution for all levels of hazard gives the damage distribution represented in blue in the 2nd quadrant. Also in the 2nd quadrant, the vulnerability function is substituted by a mean loss curve and the fragility distribution is substituted by a conditional distribution of losses, both plotted in red. The loss distribution is plotted in red in the 3th quadrant and results from the integration performed for all damage levels. To obtain the expected value of losses $E(L)$, over a given time interval, a simplification was made, namely averaging the conditional expected loss simply by the probability density function of the seismic hazard, $f_H(h)$, where:

$$E(L) = \int E(L \mid h) f_H(h)\, dh \qquad (5)$$

In each site of the analysed region, a Beta theoretical distribution was fitted to the hazard curve (Figure 3) and after being differentiated was used as the seismic hazard probability density function in Equation (5). When seismic hazard is evaluated either by an annual exceedance probability, or by an annual exceedance frequency, the latter expression describes the expected Annualized Economic earthquake Loss, previously referred to as *AEL*. Details of the approach used

to obtain the expected conditional loss $\mathrm{E}(L \mid h)$ can be found in Sousa and Campos Costa, 2015 (in this volume).

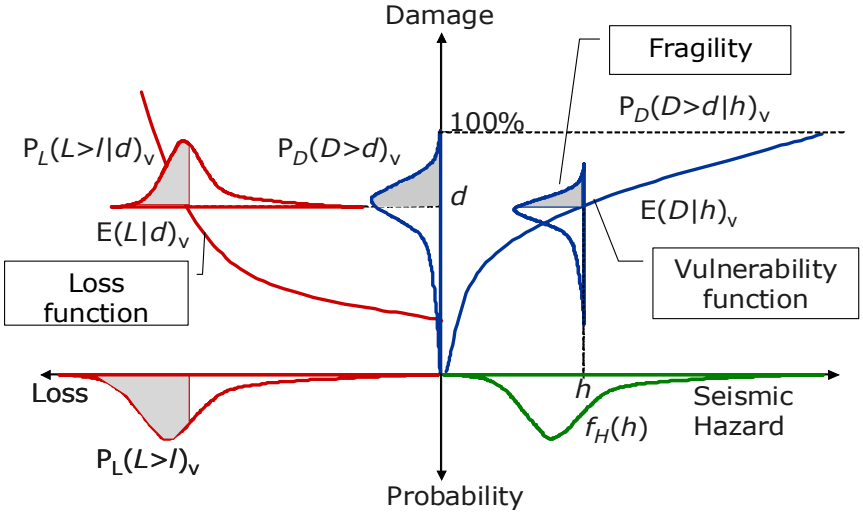

Figure 5. Schematic illustration of the seismic risk probabilistic modelling (adapted from Sousa 2008).

Following the theoretical approach shown in the previous paragraphs, it is possible to design a map summarising *AEL* for the studied region. The reference economic parameter used in calculating the estimates is the building repair cost, assumed as an average value of 200 euros per m^3 on each site of the analysis.

Figure 6 shows the risk map for the study region evaluated in terms of *AEL,* with the highest values indicated close to Santa Venerina (Linera locality on the hazard map).

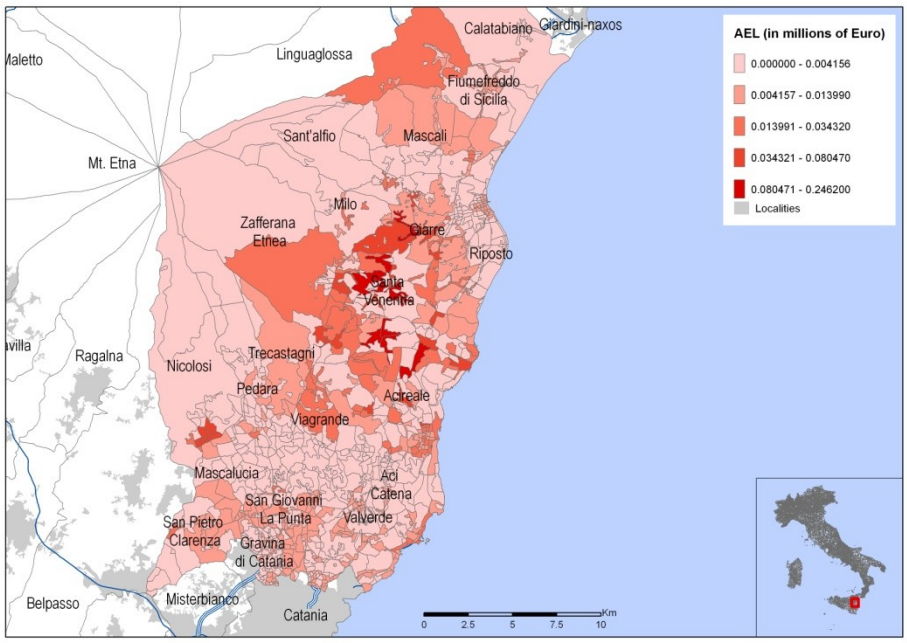

Figure 6. Risk map expressed in terms of Annualized Economic earthquake Losses (expressed in millions of Euro) for each census section of the study area.

Another possible assessment of the seismic risk of the region was obtained by evaluating the Annualized Economic earthquake Losses Ratio (*AELR*), previously defined as *AEL* normalised by the replacement value of the building inventory (FEMA, 2008). *AELR* is a useful indicator to compare relative seismic risk levels across regions. Figure 7 shows a map of *AELR* for the entire study area grouped by municipality level.

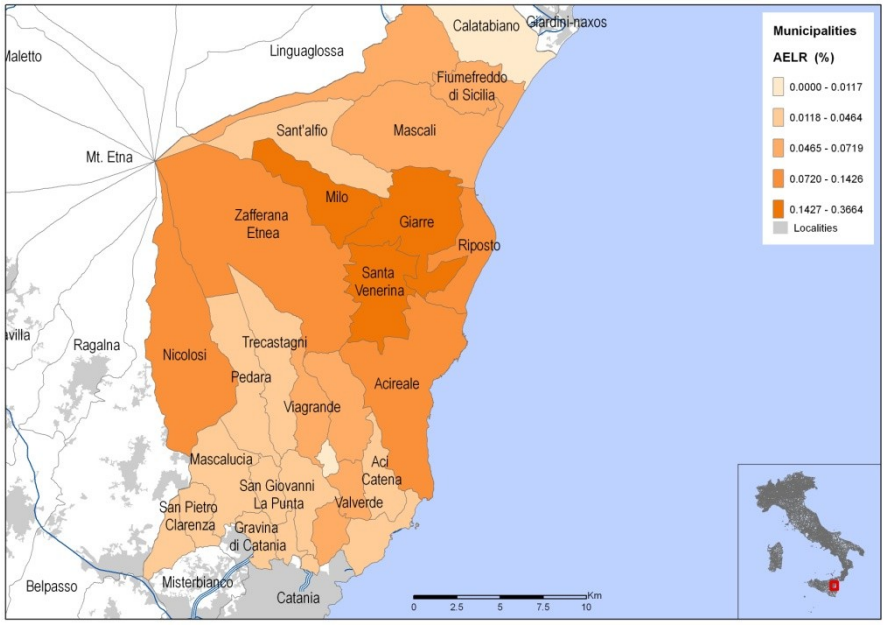

Figure 7. Risk map expressed in terms of Annualized Economic earthquake Losses Ratio (*AELR*) (in percentage) per municipality of the study area.

Table 6 shows the two interrelated risk indicators *AEL* and *AELR*, sorted from their largest values to the smallest, for each municipality of the analyzed region. Note that *AEL* and *AELR* represent the annualized losses averaged over many years and should not be compared with the impact of a single earthquake event in the region.

Table 6. Ranking Annualized Economic earthquake Losses (*AELs*) (expressed in millions of Euro) and Annualized Economic earthquake Losses Ratio (*AELRs*) (in percentage) per municipality of the Mt. Etna study area.

ISTAT code	Municipalities	AEL (M €)
19087004	Acireale	1.0671
19087017	Giarre	1.0004
19087048	S. Venerina	0.8257
19087055	Zafferana Etnea	0.3853
19087031	Nicolosi	0.3447
19087039	Riposto	0.2682
19087002	Aci Castello	0.2444
19087019	Gravina di Catania	0.2217

ISTAT code	Municipalities	AELR (%)
19087048	S. Venerina	0.3664
19087017	Giarre	0.2342
19087026	Milo	0.2239
19087055	Zafferana Etnea	0.1426
19087031	Nicolosi	0.1307
19087004	Acireale	0.1269
19087039	Riposto	0.1221
19087005	Aci S. Antonio	0.0719

ISTAT code	Municipalities	AEL (M €)
19087041	S. Giovanni la Punta	0.1930
19087024	Mascalucia	0.1846
19087023	Mascali	0.1695
19087005	Aci S. Antonio	0.1688
19087051	Tremestieri Etneo	0.1683
19087026	Milo	0.1141
19087016	Fiumefreddo di Si-cilia	0.1117
19087042	S. Gregorio di Catania	0.1104
19087034	Pedara	0.1078
19087045	S. Agata li Battiati	0.0966
19087003	Aci Catena	0.0866
19087052	Valverde	0.0759
19087053	Viagrande	0.0660
19087035	Piedimonte Etneo	0.0644
19087046	S. Alfio	0.0471
19087044	S. Pietro Clarenza	0.0460
19087050	Trecastagni	0.0383
19087012	Camporotondo Etneo	0.0193
19087010	Calatabiano	0.0123

ISTAT code	Municipalities	AELR (%)
19087016	Fiumefreddo di Sicilia	0.0669
19087035	Piedimonte Etneo	0.0601
19087052	Valverde	0.0589
19087053	Viagrande	0.0533
19087023	Mascali	0.0501
19087042	S. Gregorio di Catania	0.0487
19087044	S. Pietro Clarenza	0.0464
19087046	S. Alfio	0.0445
19087002	Aci Castello	0.0436
19087041	S. Giovanni la Punta	0.0429
19087019	Gravina di Catania	0.0418
19087024	Mascalucia	0.0357
19087045	S. Agata li Battiati	0.0349
19087050	Trecastagni	0.0331
19087051	Tremestieri Etneo	0.0315
19087003	Aci Catena	0.0296
19087012	Camporotondo Etneo	0.0285
19087034	Pedara	0.0284
19087010	Calatabiano	0.0117

5. Discussion and conclusions

This study sought to evaluate the level of seismic risk in the residential building stock of the Mt. Etna area, in Italy, taking into consideration simplified studies of the seismic hazard and vulnerability in the region.

The data on the buildings were extracted from the 1991 Italian National Institute of Statistics census. The information was grouped according to the census sections and municipalities, and the vulnerability indices were obtained using the approach proposed by Lagomarsino and Giovinazzi (2006). The damage estimated in this application refers to residential buildings.

The seismic risk was evaluated using two interrelated risk indicators, the Expected annual economic losses due to earthquakes, estimated in absolute (*AEL*) and relative (*AELR*) terms.

Some concluding observations can be made, but bearing in mind that the present work i) estimates the seismic risk related only to volcano-tectonic earthquakes of Mt. Etna and hence does not take into account the hazard related to the strong earthquakes of eastern Sicily and ii) the economic losses are exclusively based on residential building damage estimates and on the repair costs.. The municipalities of Acireale, Giarre and S. Venerina stand out for having the highest values of economic losses evaluated in absolute terms, more than twofold greater than the fourth municipality in the list, Zafferana Etnea. It is interesting to note that Giarre, Nicolosi, S. Venerina and Zafferana

Etnea retain a high standing, among the five first places of both lists of absolute and relative risk. On the other hand, Camporotondo Etneo and Calatabiano are positioned among the three last places of both lists of absolute and relative risk.

In general terms, it can be concluded that the highest values of the relative risk indicator (*AELR*) match with the hazard map of the investigated area (close to Santa Venerina; Linera locality on hazard map - Figure 2). The map of seismic risk in absolute terms (Figure 7) shows a maximum in the area of Milo, Giarre and Santa Venerina municipalities. Two zones with the same level of risk are located to east (Acireale and Riposto) and west (Zafferana Etnea), and two lower areas are located to north (Mascali and Fiumefreddo) and south (Viagrande and Valverde). The lowest values are located at the northern and southern (close to the Catania boundaries) ends of the study area.

To have an idea of the order of magnitude of the seismic risk in the Etna region, the estimates of *AELR* obtained in this study are compared with results for other locations. For instance, Sousa and Campos Costa (2015, in this volume) applied a similar approach to evaluate the seismic risk in Portugal, but used a building inventory based on more recent surveys, the Censuses 2001 and 2011. The *AELR* estimated by those authors achieved a maximum of approximately 0.3% in the southwest Portuguese counties, meaning that the highest level of the relative risk in Mt. Etna area is slightly larger than the maximum value obtained in Portugal southwest.

The results of this study may contribute to understanding the seismic risk in Mt. Etna region, both in absolute (*AEL*) and in relative (*AELR*) terms, as well as to support informed decisions on risk mitigation, addressing, for example: (i) the development of emergency plans, (ii) the planning and evaluation of costs and benefits of prevention measures, (iii) the comparisons with other risks derived from natural hazards and (iv) the prioritization of interventions to reduce the seismic risk in the region (FEMA, 2008). On the other hand, the results of this study are less useful to the insurance industry, since the risk analysis in this sector usually requires a complete treatment of uncertainty (Chen and Scawthorn, 2003). The present study does provide a long-term average of the losses due to earthquakes in any single year, but despite its probabilistic basis, did not evaluate the variance of losses.

In future, in addition to the economic effects of earthquakes, their social impacts may also be estimated, for instance, knowing the population residing in the Etna region, then the expected annualised human losses may be evaluated, as has been done by Sousa and Campos Costa (2015, in this volume).

Acknowledgements

This study was co-financed by the EU - Civil Protection Financial Instrument, in the framework the European project 'Urban Disaster Prevention Strategies using Macroseismic Fields and Fault Sources' (UPStrat-MAFA), Grant Agreement N° 23031/2011/613486/SUB/A5. Two anonymous referees are thanked for their suggestions that improved the paper.

References

Albarello D, Bramerini F, D'Amico V, Lucantoni V, Naso G (2002) Italian intensity hazard maps: a comparison of results from different methodologies. Boll Geof Teor Appl 43:249-262

Albarello D, D'Amico V, Gasperini P, Pettenati F, Rotondi R, Zonno G (2007) Nuova formulazione delle procedure per la stima dell'intensità macrosismica da dati epicentrali o da risentimenti in zone vicine. INGV-DPC Project S1, Deliverable D10. http://esse1.mi.ingv.it/d10.html

Alparone S, Maiolino V, Mostaccio A, Scaltrito A, Ursino A, Barberi G, D'Amico S, Di Grazia G, Giampiccolo E, Musumeci C, Scarfì L, Zuccarello L (2014) Instrumental seismic catalogue of Mt Etna earthquakes (Sicily, Italy): ten years (2000-2010) of instrumental recordings. Annals of Geophysics, in print

Azzaro R (2004) Seismicity and active tectonics in the Etna region: constraints for a seismotectonic model. In: Bonaccorso A, Calvari S, Coltelli M, Del Negro C, Falsaperla S (eds) Mt. Etna: Volcano Laboratory, American Geophysical Union, Geophysical monograph, 143, pp 205-220

Azzaro R, Barbano MS, D'Amico S, Tuvè T, Albarello D, D'Amico V (2008) First studies of probabilistic seismic hazard assessment in the volcanic region of Mt. Etna (Southern Italy) by means of macroseismic intensities. Boll Geof Teor Appl 49:77-91

Azzaro R, Bonforte A, Branca S Guglielmino F (2013a) Geometry and kinematics of the fault systems controlling the unstable flank of Etna volcano (Sicily). J Volcanol Geoth Res 251:5-15

Azzaro R, Castelli V (2015) Materials for an earthquake catalogue of Mt. Etna volcano from 1600 to 1831. Quaderni di Geofisica 123, 278 pp.

Azzaro R, D'Amico S, Peruzza L, Tuvè T (2013b) Probabilistic seismic hazard at Mt. Etna (Italy): The contribution of local fault activity in mid-term assessment. J Volcanol Geoth Res 251:158-169

Azzaro R, D'Amico S, Tuvè T (2015) Probabilistic seismic hazard assessment: the Mt. Etna case. Bull Earthq Eng (this volume)

Bernardini A, Giovinazzi S, Lagomarsino S, Parodi S (2007) The vulnerability assessment of current buildings by a macroseismic approach derived from the EMS-98 scale. Proceedings of the 3th Congreso Nacional de Ingenieria Sismica, Asociación Española de Ingeniería Sísmica, Girona.

Bindi D, Abdrakhmatov K, Parolai S, Mucciarelli M, Grünthal G, Ischuk A, Mikhailova N, Zschau J (2012) Seismic hazard assessment in Central Asia: outcomes from a site approach. Soil Dynamics and Earthquake Engineering 37:84-91

Chen, W.F. & Scawthorn, C., (2003).Earthquake Engineering Handbook. CRC Press.

CMTE Working Gropu (2014) Catalogo Macrosismico dei Terremoti Etnei dal 1832 al 2013. INGV Catania. http://www.ct.ingv.it/macro

Crowley H, Colombi M, Borzi B, Faravelli M, Onida M, Lopez M, Polli D, Meroni F, Pinho R (2009) A comparison of seismic risk maps for Italy. Bull Earthq Eng 7:149–180

D'Amico V, Albarello D (2003) Seismic hazard assessment from local macroseismic observation: comparison with a "standard" approach. Natural Hazards 29:77-95

D'Amico V, Albarello D (2008) SASHA: a computer program to assess seismic hazard from intensity data. Seismol Res Lett 79:663-671

FEMA (2008) HAZUS MH Estimated annualized earthquake losses for the United States. FEMA 366, Federal Emergency Management Agency Mitigation Directorate. Washington DC., U.S.A.

Frassine L, Giovinazzi S (2004) Basi di dati a confronto nell'analisi di vulnerabilità sismica dell'edilizia residenziale: un'applicazione per la città di Catania. Proceedings of the XI Congresso Nazionale "L'ingegneria Sismica in Italia", Genova, Italy

Galea P (2007) Seismic history of the Maltese islands and considerations on seismic risk. Annals of Geophysics 50:725-740

Giovinazzi S, Lagomarsino S (2001) Una metodologia per l'analisi di vulnerabilità sismica del costruito. Proceedings of the X Congresso Nazionale "L'ingegneria Sismica in Italia", Potenza-Matera, CD-ROM

Grünthal G (eds) (1998) European Macroseismic Scale 1998 (EMS-98). European Seismological Commission, Subcommission on Engineering Seismology, Working Group Macroseismic Scale. Conseil de l'Europe, Cahiers du Centre Européen de Géodynamique et de Séismologie, 15, Luxembourg, pp. 99. http://www.ecgs.lu/cahiers-bleus/

ISTAT (1991) 13° censimento generale della popolazione, 1991. Dati sulle caratteristiche strutturale della popolazione e delle abitazioni, Roma.

Lagomarsino S, Giovinazzi S (2006) Macroseismic and mechanical models for the vulnerability and damage assessment of current buildings. Bull Earthq Eng 4:415-443

Lo Giudice E, Patanè G, Rasà R, Romano R (1982) The structural framework of Mount Etna. Memorie Società Geologica Italiana 23:125-158

Lo Giudice E, Rasà R (1992) Very shallow earthquakes and brittle deformation in active volcanic areas: the Etnean region as example. Tectonophysics 202:257-268

McGuire WJ, Pullen AD (1989) Location and orientation of eruptive fissure and feeder-dykes at Mount Etna; influence of gravitational and regional tectonic stress regimes. J Volcanol Geoth Res 38:325-344

Meroni F, Petrini V, Zonno G (1999) Valutazione della vulnerabilità di edifici su aree estese tramite dati ISTAT. Proceedings of the IX Congresso Nazionale "L'ingegneria Sismica in Italia", Torino, CD-ROM.

Meroni F, Petrini V, Zonno G (2000) Distribuzione nazionale della vulnerabilità media comunale. In: Bernardini A (ed) La vulnerabilità degli edifici, CNR-GNDT, Roma, pp 105-131

Meroni F, Zonno G, Azzaro R, D'Amico S, Tuvè T, Oliveira CS, Ferreira MA., Mota de Sá F, Brambilla C, Rotondi R, Varini E (2015) The role of the urban system dysfunction in the assessment of seismic risk in the Mt. Etna area (Italy). Bull Earthq Eng 13 (6) doi 10.1007/s10518-015-9780-8

Monaco C, Tapponnier P, Tortorici L, Gillot PY (1997) Late quaternary slip rate on the Acireale-Piedimonte normal faults and tectonic origin of Mt. Etna (Sicily). Earth and Planetary Science Letters 147:125-139

Mucciarelli M, Peruzza L, Caroli P (2000) Tuning of seismic hazard estimated by means of observed site intensities. Journal of Earthquake Engineering 4:141-159

Rovida A, Camassi R, Gasperini P, Stucchi M (eds.) (2011) CPTI11, the 2011 version of the Parametric Catalogue of Italian Earthquakes. Milano, Bologna. DOI: 10.6092/INGV.IT-CPTI11. http://emidius.mi.ingv.it/CPTI

Sousa ML (2008) Annualized Economic and Human Earthquake Losses for Mainland Portugal. 14th World Conference on Earthquake Engineering, Beijing, China

Sousa ML, Campos Costa A (2015) Evolution of earthquake in Portuguese residential building stock, Bull Earthq Eng (this volume)

Zonno G, Azzaro R et al. (2012) Urban Disaster-Prevention Strategies Using Macroseismic Fields and Fault Sources. 15th World Conference on Earthquake Engineering, Lisbon, Portugal. http://www.iitk.ac.in/nicee/wcee/article/WCEE2012_0678.pdf